

# Vertical bounce of two vertically aligned balls

Rod Cross<sup>a)</sup>

Department of Physics, University of Sydney, Sydney NSW 2006, Australia

(Received 26 April 2007; accepted 14 July 2007)

When a tennis ball rests on top of a basketball and both drop to the floor together, the tennis ball is projected vertically at high speed. A mass-spring model of the impact, as well as air track data, suggest that the tennis ball should be projected at relatively low speed. Measurements of the forces on each ball and the bounce of vertically aligned superballs are used to resolve the discrepancy.

© 2007 American Association of Physics Teachers.

[DOI: 10.1119/1.2772286]

## I. INTRODUCTION

A popular demonstration is to drop a basketball on the floor with a tennis ball on top of the basketball.<sup>1-4</sup> The tennis ball bounces off the basketball at surprisingly high speed. The usual explanation involves two steps. First, the basketball bounces off the floor and reverses direction. Then the basketball collides with the tennis ball and projects the tennis ball toward the ceiling. If there is no loss of energy and if the two balls fall to the floor at speed  $v$ , the basketball bounces at speed  $v$  and collides with the incoming tennis ball. Relative to the basketball, the tennis ball is incident at speed  $2v$  and bounces off the basketball at a speed of about  $2v$ . But the basketball is rising at speed  $v$  so the tennis ball is projected vertically at about  $3v$  and bounces to about nine times the drop height. Given that a tennis ball normally bounces to about 0.55 of its drop height, it gains about 16 times more energy by bouncing off the basketball than it does by bouncing off the floor.

This explanation is plausible and is also roughly consistent with observations. The actual bounce speed is closer to  $2v$  than  $3v$  due to energy losses. Nevertheless, the usual explanation ignores the facts that the two balls remain in contact during the collision, and the manner in which the energy is shared between the two balls depends on their relative stiffness. Furthermore, this explanation is not generally consistent with similar observations. An equivalent experiment was performed by the author using two masses on an air track. The two masses can be projected toward the end stop while in contact with each other, or they can be projected at the same speed and spaced a short distance apart. The first arrangement simulates the drop of two balls in contact. The second arrangement simulates the situation commonly used to explain the result.

An advantage of using an air track with soft springs attached to each mass and to the end stop is that the collision process is slow enough at low launch speeds to be observed by eye. An additional advantage is that the relative stiffness of each pair of springs is a known quantity. They have the same stiffness. If the masses remain in contact before the collision, they remain in contact during the collision with the end stop and then reflect off the end stop at similar speeds, regardless of the mass ratio. If the masses are incident at the same speed but are spaced apart, the results are different.<sup>5</sup> The mass colliding with the end stop reflects off the stop, then collides with the second mass, and depending on the mass ratio, can come to a complete stop. Alternatively, it can reflect backward off the second mass, reflect off the end stop, and then collide again with the second mass and come to a

complete stop. If one of the masses comes to a stop, the other acquires the total incident energy of the two separate masses. An experimental and theoretical study of these effects is presented in the following.

## II. COLLISION MODELS

Suppose that masses  $m_1$  and  $m_2$  are each headed toward the end stop of an air track, at speed  $v_0$  as shown in Fig. 1(a). The masses are not in contact initially. When mass  $m_1$  collides with the end stop, it reflects at speed  $ev_0$  where  $e$  is the coefficient of restitution. For simplicity we assume that  $e$  is the same when  $m_1$  collides with  $m_2$ . The collision shown in Fig. 1(b) results in a change in speed of both masses, as shown in Fig. 1(c). Using conservation of momentum and the definition of  $e$ , we find that

$$\frac{v_1}{v_0} = \frac{em_1 - (1 + e + e^2)m_2}{m_1 + m_2}, \quad (1)$$

$$\frac{v_2}{v_0} = \frac{e(2 + e)m_1 - m_2}{m_1 + m_2}. \quad (2)$$

Figure 2(a) shows  $v_1/v_0$  and  $v_2/v_0$  versus  $m_1/m_2$ . Mass  $m_1$  comes to rest with  $v_1=0$  if  $m_1=(1+e+e^2)m_2/e$ . This condition is satisfied closely when  $m_1=3m_2$ , regardless of the value of  $e$ . For example, if  $e=1$ , then  $m_1=3m_2$ , and if  $e=0.8$ , then  $m_1=3.05m_2$ . If  $v_1=0$  and  $e=1$ , then  $v_2=2v_0$ , indicating that all the initial energy is transferred to  $m_2$ . If  $m_1 \gg m_2$ , then  $v_2=e(2+e)v_0$  and  $v_1=ev_0$ .

If  $m_1 < 3m_2$ , then  $m_1$  bounces backward off  $m_2$  with  $v_1 < 0$ , as shown in Fig. 1(d). In this case,  $m_1$  bounces off the end stop a second time and approaches  $m_2$  at speed  $ev_1$ , as shown in Fig. 1(e). If  $ev_1 < v_2$ , there is no further collision. However, if  $ev_1 > v_2$ , then  $m_1$  will catch up with  $m_2$  and undergo a second collision. The latter situation arises when  $m_1 < m_2$ . The result of the second collision is shown in Fig. 1(f) and is given by

$$v_3 = \frac{(1 + e)m_2v_2 + e(em_2 - m_1)v_1}{m_1 + m_2}, \quad (3)$$

$$v_4 = \frac{(m_2 - em_1)v_2 - e(1 + e)m_1v_1}{m_1 + m_2}, \quad (4)$$

where  $v_1$ , defined by Eq. (1), is negative. Figure 2(b) shows the result of the second collision. In this case,  $m_1$  comes to rest when  $m_1$  is  $\approx 0.52m_2$ . The result of additional collisions between the two masses, which arise if  $m_1$  is smaller than

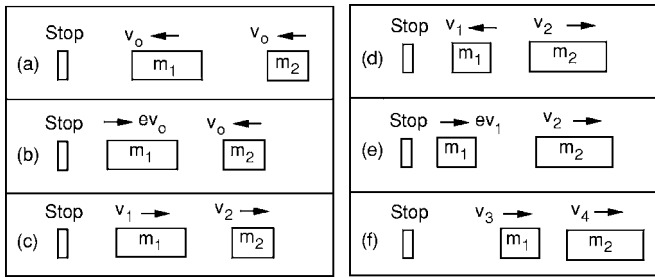


Fig. 1. (a) Two masses headed toward the end stop of an air track at the same speed  $v_0$ . (b) Mass  $m_1$  reflects at speed  $ev_0$  and collides with  $m_2$ . If  $m_1 > 3m_2$ ,  $m_1$  continues to the right at reduced speed  $v_1$  as in (c); otherwise it comes to a stop or heads back to the end stop as in (d). The subsequent behavior is shown in (e) and (f).

about  $4m_2$ , can be determined by repeated application of Eqs. (3) and (4). Experimental results showing multiple collisions are described in Sec. IV.

If the two masses (or two balls) remain in contact when incident at speed  $v_0$ , and also remain in contact during the collision with the end stop (or the floor), then the situation can be analyzed by referring to Fig. 3. Mass  $m_1$  impinges on the end stop via a linear spring  $S_1$  of spring constant  $k_1$  attached either to  $m_1$  or to the end stop. The masses  $m_1$  and  $m_2$  are separated by a linear spring  $S_2$  of spring constant  $k_2$  attached either to  $m_2$  or  $m_1$  but not to both. Springs  $S_1$  and  $S_2$

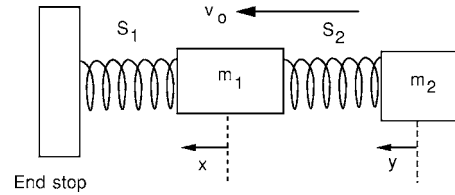


Fig. 3. If  $m_1$  remains in contact with the end stop and with  $m_2$  during the collision, the collision can be analyzed using connecting springs  $S_1$  and  $S_2$ . The same situation arises when one ball sits on another and both fall to the floor together.  $x$  and  $y$  denote the displacements of the two masses.

can compress but they cannot extend. Let  $x$  be the coordinate of the center of mass of  $m_1$  and  $y$  be the coordinate of the center of mass of  $m_2$ , in which case the compression of  $S_1$  can be equated to  $x$  and the compression of  $S_2$  is  $y-x$ . While the springs remain compressed, the equations of motion are

$$m_1 \frac{d^2x}{dt^2} = F_1 = k_2(y-x) - k_1x, \quad (5)$$

$$m_2 \frac{d^2y}{dt^2} = F_2 = -k_2(y-x), \quad (6)$$

where  $F_1$  and  $F_2$  are the forces on each mass. Equations (5) and (6) can be integrated numerically with initial conditions  $y=x=0$  and  $dx/dt=dy/dt=v_0$ . If the masses are incident at the same speed but separated by a distance  $d$ , we can start the integration with  $x=0$  and  $y=-d$ . By varying  $d$ , it is possible to study the continuous transition between the separate (large  $d$ ) and the simultaneous ( $d=0$ ) collision models. We assume for now that  $d=0$ . If at any subsequent time  $x < 0$ , then  $k_1 = 0$ . Similarly, if  $y-x < 0$ , then  $k_2 = 0$ . The integration can be terminated when  $k_1$  and  $k_2$  are both zero, at which time  $m_1$  recoils at speed  $v_1$  and  $m_2$  recoils at speed  $v_2$ . However, if  $v_1 > v_2$ , then a second collision between  $m_1$  and  $m_2$  will occur, in which case the integration needs to be continued to determine the outcome.

Solutions of Eqs. (5) and (6) are shown in Fig. 4 for two different values of the stiffness ratio  $r_k = k_1/k_2$ . The results in Fig. 4(a) (with  $r_k=1$ ) are quite different from those in Fig. 2, even for cases where  $e=1$ , and hence where there is no loss of energy. The results in Fig. 4(b) (with  $r_k=20$ ) are similar to those in Fig. 2, but not identical. The numerical solutions were checked to ensure that the total energy was conserved during and after the collision. The results described here are consistent with those obtained by Patricio<sup>6</sup> who used a nonlinear rather than a linear spring model to describe an essentially identical problem regarding collisions between elastic spheres. The differences between the separate and the simultaneous collision models are therefore related to the magnitude of  $r_k$  rather than the nonlinearity of the springs of the colliding masses.

Given that energy is conserved in both sets of calculations, we might expect an identical set of results. However, the manner in which energy is shared between the two masses depends on the mass ratio  $r_m = m_1/m_2$  and the stiffness ratio,  $r_k = k_1/k_2$ . It is only when  $r_k \gg 1$  that the two models of the collision agree. The solutions in Fig. 4(b) with  $r_k=20$  are therefore approximately the same as those in Fig. 2. When  $r_k$  is large, the time scale for a collision between  $m_1$  and the end stop is much shorter than that between  $m_1$  and  $m_2$ . In effect, these collisions are two separate events and can therefore be

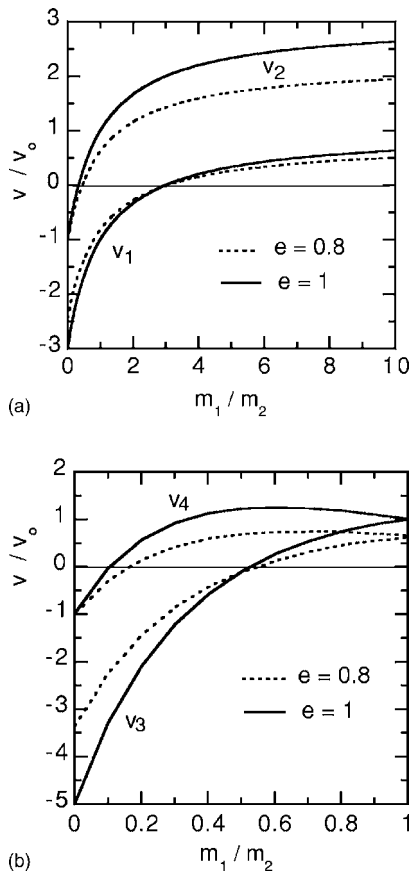


Fig. 2. (a) The ratios  $v_1/v_0$  and  $v_2/v_0$  versus  $m_1/m_2$  for  $e=0.8$  or  $1.0$ . If  $v_1 < 0$ ,  $m_1$  reflects off the end stop a second time at speed  $ev_1$ . (b) The ratios  $v_3/v_0$  and  $v_4/v_0$  versus  $m_1/m_2$  for  $e=0.8$  or  $1.0$ . These solutions apply when  $m_1 < m_2$ . If  $v_3 < 0$ ,  $m_1$  reflects off the end stop a third time at speed  $ev_3$ .

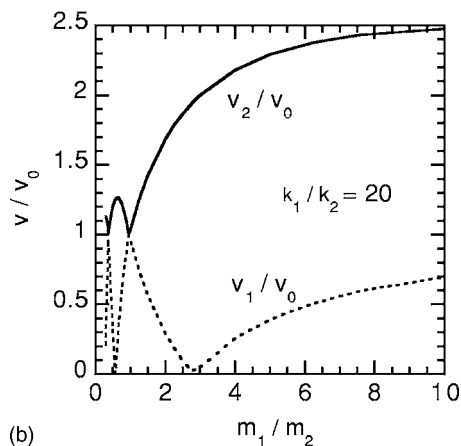
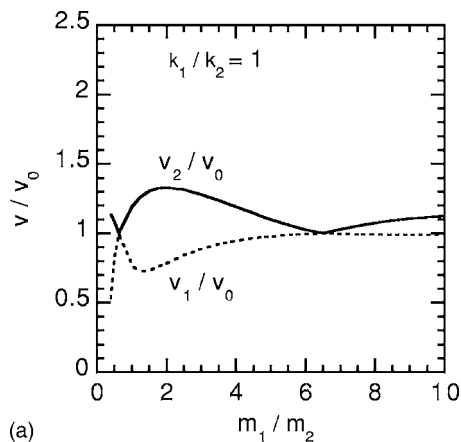


Fig. 4. Solutions of Eqs. (5) and (6) when (a)  $k_1/k_2=1$  and (b)  $k_1/k_2=20$ .

approximated as such. Solutions of Eqs. (5) and (6) with  $r_m=2$  and  $r_k=20$  are shown in Fig. 5 to illustrate this point. The two separate collisions of  $m_1$  with the end stop are easily recognized. In the time  $t < 5$  ms,  $m_1$  collides with the end stop and reverses direction while  $m_2$  continues toward the end stop with almost no change in speed. In the interval  $5 < t < 19$  ms, there is a slow collision between  $m_1$  and  $m_2$

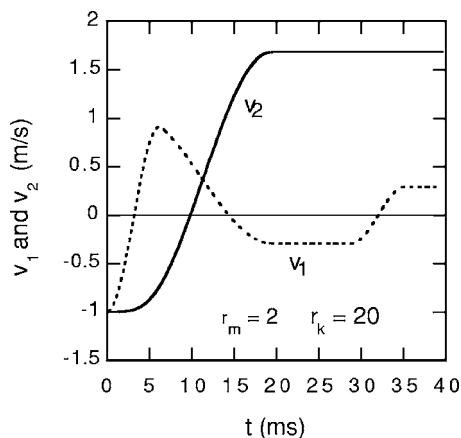


Fig. 5. Solutions of Eqs. (5) and (6) with  $m_1=0.4$  kg,  $m_2=0.2$  kg,  $k_1=1 \times 10^5$  N m<sup>-1</sup>, and  $k_2=5 \times 10^3$  N m<sup>-1</sup>. During the interval  $19$  ms  $< t < 29$  ms,  $m_1$  travels back toward the end stop at constant speed, and  $m_2$  travels away from the end stop at constant speed.

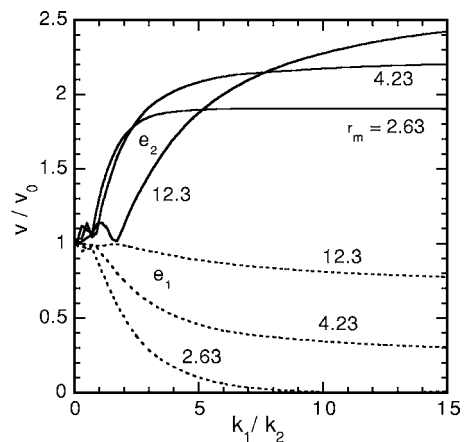


Fig. 6. Rebound speed ratios  $e_1=v_1/v_0$  (dashed curves) and  $e_2=v_2/v_0$  (solid curves) versus the stiffness ratio  $r_k$  for three values of the mass ratio  $r_m$ .

causing both masses to reverse direction. The mass  $m_1$  makes a second collision with the end stop after 29 ms, but does not subsequently catch up to  $m_2$ .

If  $k_1$  and  $k_2$  are similar in magnitude, the collisions of  $m_1$  with the end stop and with  $m_2$  can no longer be described as separate events. The outcome of any particular collision is then surprisingly difficult to predict, even for the simplest case where  $m_1=m_2$ ,  $k_1=k_2$ , and  $v_0=1$  m/s. If treated as separate events, we would expect  $m_1$  to reflect off the end stop at 1 m/s, then reflect off  $m_2$  back toward the end stop at 1 m/s, and then reflect again off the end stop at 1 m/s, while  $m_2$  would reflect just once off  $m_1$  at 1 m/s. If equal masses are connected by equal springs then  $m_2$  reflects off  $m_1$  at 1.19 m/s while  $m_1$  reflects off the end stop at 0.76 m/s.

Figure 6 shows the rebound speeds of the two masses as a function of  $r_k$  for three values of the mass ratio relevant to the experiments described in Secs. III and IV. When  $k_1$  and  $k_2$  are about equal, both masses rebound at relatively low speed, regardless of the mass ratio, which is the result when two masses are incident in contact with each other on an air track. In order for mass  $m_2$  to rebound at high speed,  $r_k$  needs to be comparable to or greater than the mass ratio. The latter result implies that the collision time between  $m_1$  and the end stop needs to be smaller than the collision time between  $m_1$  and  $m_2$ . That is,  $m_1/k_1 < m_2/k_2$  (approximately).

When  $k_1$  and  $k_2$  are about equal, large differences arise between the two collision models at large  $r_m$ , representing the expected situation where a tennis ball is on top of a basketball and both are dropped together to the floor. For example, we see from Fig. 2 that the tennis ball will bounce at  $2.64v_0$  if  $m_1/m_2=10$ , but the spring model indicates that the tennis ball should bounce at  $1.13v_0$  when  $r_m=10$  and  $r_k=1$ . This result suggests that the high speed bounce of a tennis ball resting on a basketball might be the result of a physical separation between the two balls as they fall to the floor. Alternatively, the stiffness between the two balls might be significantly smaller than the stiffness between the basketball and the floor, or there might be some other effect that contributes to the high rebound speed of the tennis ball, such as rapid vibration of the upper surface of the basketball. To investigate the discrepancy, the result of dropping a basketball and a tennis ball together was examined experimentally, as described in Sec. III. Additional experiments using two superballs are described in Sec. IV.

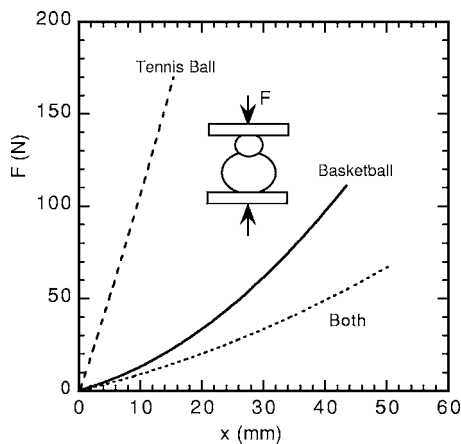


Fig. 7. Force versus compression measured under static conditions for each ball separately and with one on top of the other as shown in the inset.

### III. BASKETBALL AND TENNIS BALL EXPERIMENT

A tennis ball of mass 57 g and diameter 66 mm was balanced by hand on top of a small basketball of mass 150 g and diameter 160 mm and dropped from a height of 0.71 m onto a hard floor. The impact was filmed and examined frame by frame. Dropped separately, the basketball bounced to a height of 0.42 m and the tennis ball bounced to a height of 0.40 m. Dropped together, the two balls appeared to remain in contact before reaching the floor. The basketball bounced to a height of only about 0.01 m and the tennis ball bounced to a height of  $1.72 \pm 0.03$  m. The tennis ball was incident at  $v_0 = 3.53$  m/s as the two balls impacted the floor, and bounced at  $v_2 = 5.8$  m/s, with a velocity ratio  $v_2/v_0 = 1.64$ . The two balls were incident with a total energy of 1.29 J. The energy remaining after the collision was 0.96 J. Dropped side by side rather than one on top of the other, the energy remaining was 0.84 J. The vertical stacking arrangement was therefore slightly more energy efficient in terms of the overall energy loss, a result that can be attributed to the softer impact of the tennis ball. In the same way, a tennis ball bouncing off the strings of a clamped racquet bounces higher than off a hard floor, due to the softer impact on the strings.<sup>7</sup>

The mass ratio in the experiment was  $m_1/m_2 = 2.63$ . The stiffness of each ball was measured under static conditions using a materials testing machine, and the results are shown in Fig. 7. Each test was conducted by compressing the balls between parallel metal plates. The compression curves are slightly nonlinear but can be approximated by a linear fit to estimate the impact duration and the force on each ball. At a compression force of 30 N, the basketball compressed by 18.6 mm, the tennis ball compressed by 2.9 mm, and the two in series compressed by 27.7 mm. The series compression was 6.2 mm greater than the combined individual compressions because the tennis ball acted to concentrate the load force locally at the top of the basketball, resulting in a local indentation of the basketball as shown by the inset in Fig. 7. If we assume in the latter case that the bottom of the basketball compressed by 9.3 mm (half the total compression of the basketball alone) and the tennis ball compressed by 2.9 mm, then the top of the basketball compressed by 15.5 mm. In terms of the model shown in Fig. 3,  $k_1/k_2 = 1.8$  for this data.

The dynamic values of the ball stiffness in Eqs. (5) and (6)

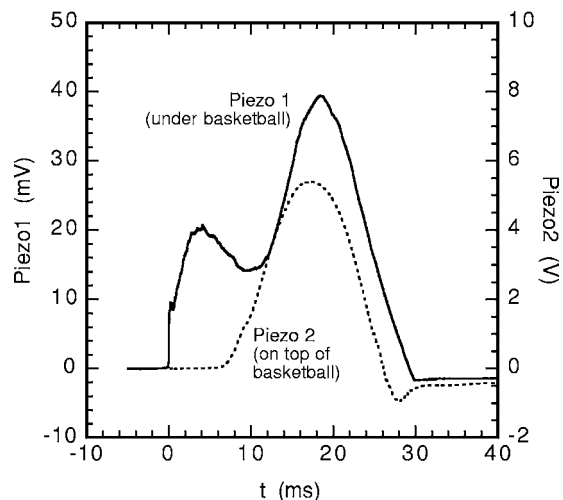


Fig. 8. Force waveforms measured when a tennis ball is on top of a basketball and when both are dropped to the floor. The piezoelectric P1 on the floor generates a voltage proportional to force on the bottom of the basketball. The P2 signal is proportional to the force between the two balls.

refer not to static compression but to the displacement of the center of mass of each ball. Because the displacement of the center of mass of a ball during a bounce is less than its overall compression under static loading conditions, the dynamic stiffness of a ball is larger than its static value.<sup>8</sup> For example, the static stiffness of the tennis ball at  $F = 30$  N was  $1.03 \times 10^4$  N m<sup>-1</sup>. The dynamic stiffness of a ball,  $k_d$ , can be estimated from its impact duration  $\tau = \pi\sqrt{m/k_d}$ .<sup>8,9</sup> For a 57 g tennis ball impacting on a heavy, rigid surface,  $\tau = 5.0$  ms, so  $k_d = 2.25 \times 10^4$  N m<sup>-1</sup>.

Figure 8 shows a qualitative measurement of the forces acting on the two balls. The two balls were dropped together onto an 8 mm thick, 50 mm diameter ceramic piezoelectric disk (P1) attached to a heavy metal plate on the floor. A 0.3 mm thick, 15 mm diameter piezoelectric disk (P2) was taped to the top of the basketball, with the tennis ball resting on top of P2. P2 was about 20 times more sensitive than P1 in terms of its output voltage for a given applied force. The two balls were dropped from a height of about 30 cm. P1 generated a voltage signal proportional to the force on the bottom of the basketball. P2 generated a signal proportional to the force between the two balls. The raw signals were not calibrated, but show that the impact duration was 30 ms, there is essentially no force between the two balls for the first 7 ms, and the initial impact results in a rapid increase in the force at the bottom of the basketball. The rapid increase in the force can be explained in terms of the short time delay for the bottom of a hollow ball to buckle.<sup>9</sup> Before that time, the ball is dynamically very stiff, but after that time the ball is relatively soft. The P1 waveform indicates that there are two separate peaks, but this result is spurious and arises from the fact that the contact diameter of the basketball on the floor is greater than 50 mm (the diameter of P1). When the bottom of the basketball buckles, the central part of the contact area rises up off P1.<sup>9</sup> The P1 waveform is reliable only at the beginning and end of the bounce while the contact area remains less than 50 mm.

According to Eqs. (1) and (2), a lossless ( $e = 1$ ) basketball would bounce with  $v_1 = 0.36$  m/s and a lossless tennis ball would bounce with  $v_2 = 6.70$  m/s when  $m_1/m_2 = 2.63$ , and

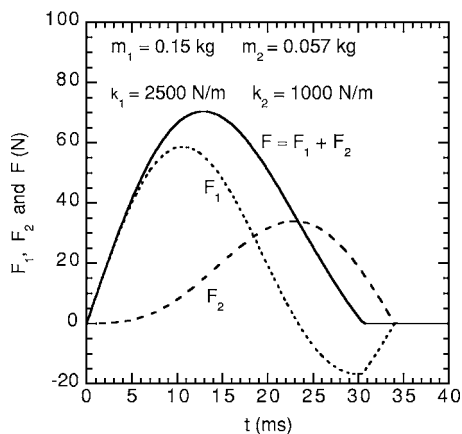


Fig. 9. A solution of Eqs. 5 and 6 approximating the experimental results in Fig. 8.

$v_0=3.53$  m/s. When  $e=0.9$ ,  $v_1=0.33$  m/s, and  $v_2=5.70$  m/s. Experimentally,  $v_1=0.44$  m/s, and  $v_2=5.8$  m/s. Equations (1) and (2) with  $e=0.9$  therefore provide a good description of the experimental results, despite the fact that the two balls did not appear to separate as they fell. The measured impact duration was 30 ms, so the two balls (incident at 3.53 m/s) would need to be separated by at least 106 mm if the basketball were to collide first with the floor and then with the tennis ball. In reality, the two balls were separated by 2 mm at most, so the analysis based on Eqs. (1) and (2) is inappropriate and the good agreement appears to be fortuitous.

A poor fit to the data in Fig. 8 is obtained with the two-spring model using the previously mentioned static stiffness parameters, the problem being that the calculated impact duration would be 39 ms. The dynamic stiffness of at least one of the balls is therefore larger. A better fit to the data is obtained using the parameters  $k_1=2500$  N m<sup>-1</sup> and  $k_2=1000$  N m<sup>-1</sup>. The result of this calculation is shown in Fig. 9. The corresponding rebound speeds are  $v_1=1.34$  m/s and  $v_2=6.37$  m/s, both being higher than observed. If energy losses in the two springs were included in the model, it would presumably be possible to obtain even better agreement with the experimental data. For example, a plausible result is obtained by multiplying  $v_2$  by 0.9, representing the effective coefficient of restitution between the two balls.

The solution in Fig. 9 shows that there is a delay of about 5 ms before  $F_2$  begins to increase, in qualitative agreement with the experimental result in Fig. 8. An alternative fit with  $k_1=2000$  N m<sup>-1</sup> and  $k_2=500$  N m<sup>-1</sup> also gives the desired 30 ms impact duration, and a better result where the basketball bounces to a height of only 19 mm (with  $v_1=0.61$  m/s), but the force  $F_2$  between the two balls does not drop to zero until 43 ms due to the low value of  $k_2$ .

#### IV. EXPERIMENTS WITH SUPERBALLS

A similar experiment to that described in Sec. III was repeated using three superballs to minimize the effects of energy loss in each ball and to ensure that the contact area of the ball on P1 did not extend beyond the edge of the disk. The properties of each ball are listed in Table I. The parameter  $\tau$  and COR are the impact duration and coefficient of restitution of each ball dropped from a height of 20 cm onto P1 mounted on a heavy metal plate,  $k_s$  is the static stiffness

Table I. Superball properties.  $D$  is the ball diameter,  $m$  is the ball mass, and COR is the coefficient of restitution.

Ball	$D$ (mm)	$m$ (g)	$k_s$ (N m <sup>-1</sup> )	$\tau$ (ms)	$k_d$ (N m <sup>-1</sup> )	COR
B1	58	101	$4 \times 10^4$	4.3	$5.4 \times 10^4$	0.78
B2	38	24.8	$1.3 \times 10^4$	2.6	$3.6 \times 10^4$	0.90
B3	26	8.5	$1.2 \times 10^4$	1.9	$2.3 \times 10^4$	0.90

measured in a materials testing machine, and  $k_d$  is the dynamic stiffness calculated from the relation  $\tau = \pi \sqrt{m/k_d}$ . The experimental error in  $\tau$  is  $\pm 0.1$  ms. The error in the coefficient of restitution is  $\pm 0.02$ . The error in  $m$  is  $\pm 0.02$  g and the error in  $k_s$  is  $\pm 5\%$ .

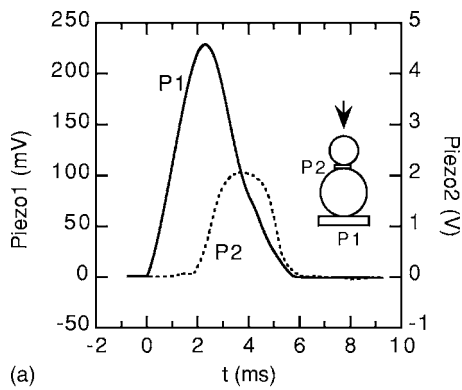
To a good approximation, the dynamic stiffness of the three balls is proportional to the ball radius, indicating that for any given dynamic compression of a ball, the contact area is proportional to the ball radius (assuming that the compressed volume is approximately cylindrical). The same relation is found when two identical steel balls collide. Hessel *et al.*<sup>10</sup> report data on the collision times of two steel balls of diameter 38.1 mm and another two of diameter 27.0 mm. The ratio of the diameters is 1.411, the ratio of the collision times was 1.407, and the ratio of the masses was 2.815. The ratio of the dynamic stiffness values was therefore  $2.815/1.407^2=1.422$ , essentially the same as the ratio of the ball diameters.

In each of the following experiments, two of the balls were aligned vertically and dropped from a height  $h_0$  of about 20 cm. That is, the bottom of the lower ball was about 20 cm above P1. Each bounce was filmed at 25 frames/s with a video camera for later analysis. A summary of each experiment is given in Table II in terms of the quantities  $e_1=v_1/v_0$  and  $e_2=v_2/v_0$ , where  $v_0$  is the common speed of the two incident balls,  $v_1$  is the rebound speed of the bottom ball, and  $v_2$  is the rebound speed of the top ball. The errors in  $e_1$  and  $e_2$  were  $\pm 0.02$  averaged over three or four “good” bounces. It was difficult to keep the ball centers perfectly aligned, especially with the small ball out of view under the large ball, with the result that the balls did not always bounce vertically. Bounces that were more than  $10^\circ$  away from the vertical were disregarded. Also shown in Table II are the bounce height to drop height ratios  $h_1/h_0=e_1^2$  and  $h_2/h_0=e_2^2$ .

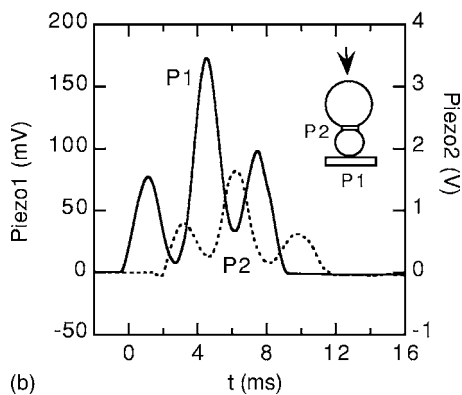
With B2 on top of B1, the small ball (B2) bounced 3.65 times higher than the drop height and the large ball bounced to 8% of its drop height. The force on the bottom of the larger ball was measured with P1 and the force on the smaller ball was measured with P2. In this case, P2 was taped to a 28 mm diameter, 2 mm thick flat disk glued to a

Table II. Values of  $e_1$  and  $e_2$ , for each ball pair. Bottom (top) refers to the bottom (top) ball. The last entry is the result for the tennis ball on top of the basketball.

Bottom	Top ( $m_2$ )	$m_1/m_2$	$e_1$	$e_2$	$h_1/h_0$	$h_2/h_0$
B1	B2	4.23	0.28	1.91	0.08	3.65
B2	B1	0.236	0.17	0.84	0.033	0.71
B1	B3	12.3	0.68	2.26	0.46	5.11
B3	B1	0.081	0.51	0.70	0.26	0.49
B1	B1	1.040	0.76	0.76	0.58	0.58
150 g	57 g	2.63	0.18	1.64	0.03	2.69



(a)



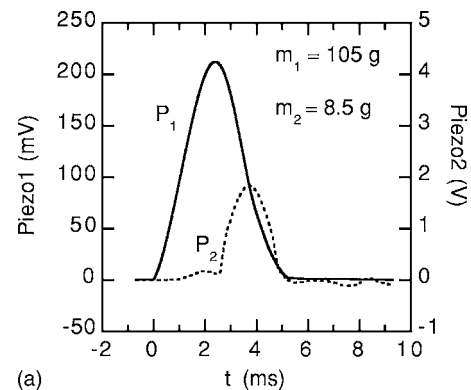
(b)

Fig. 10. (a) Force waveforms measured with ball B2 on top of B1 and when both were dropped together. P1 generates a voltage proportional to the force on the bottom of the bottom ball. The P2 signal is proportional to the force between the two balls. (b) Result when B1 is on top of B2.

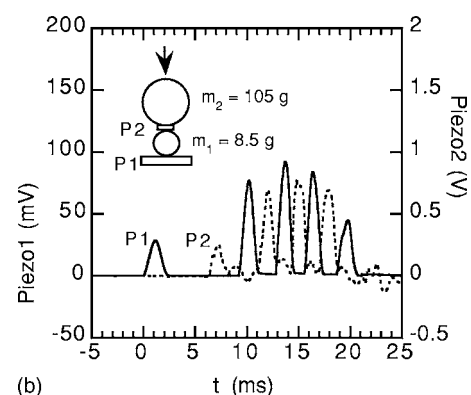
30 mm diameter flat section ground on the larger ball. The purpose of the latter arrangement was to eliminate any response from P2 due to bending. The result of this measurement is shown in Fig. 10(a). The two balls together bounced with an impact duration of 6.0 ms. When the larger ball was dropped with the smaller ball underneath, the impact duration extended to 9.0 ms, as indicated by the results shown in Fig. 10(b). With the ball positions reversed, the large ball bounced to 71% of its drop height and the small ball bounced to only 3.3% of its drop height.

If we assume that the balls undergo separate collisions, a good fit to the data can be obtained with  $e=0.90$ . With B2 on top of B1, Eqs. (1) and (2) indicate that B2 should bounce to 3.68 times the drop height and B1 should bounce to 4% of its drop height. With B1 on top, repeated application of Eqs. (3) and (4) show that there are three collisions between the two balls before B1 bounces to 59% of the drop height and B2 bounces to essentially zero height. A better fit in the latter case is obtained with  $e=0.92$  in which case there are still three bounces before the large ball bounces to 71% of the drop height (as observed) and the small ball bounces to 0.1% of the drop height.

Figure 10(b) shows the three collisions. The collisions are qualitatively consistent with there being a physical separation between the two balls while the small ball bounces up and down three times between the large ball and P1. In reality, the collisions overlap in Fig. 10(b), indicating that the small ball is effectively connected by a spring to both the large ball and P1, the spring being the ball itself. Regardless of whether the small or large ball was on top, there was a



(a)



(b)

Fig. 11. (a) Force waveforms measured when the small superball B3 is on top of B1 and when both are dropped together. The P2 response from 0 to 2.5 ms and at  $t > 5$  ms was also present when B1 was dropped on its own and is due to vibration of the upper surface of B1. (b) Result when B1 is on top of B3.

delay of about 2 ms before the two balls made initial contact, as recorded by P2, indicating that the two balls were separated by about 1 mm as they fell.

To investigate further, the experiment was repeated using B1 and B3, and the results are shown in Fig. 11. The delay in Fig. 11(a) was also about 2 ms, but the delay in Fig. 11(b) was about 7 ms. By repeating the drop with the small ball underneath, it was possible to reduce the delay to 2 ms on occasion, in which case the last four P2 peaks shown in Fig. 11(b) merged into one broad peak with four small subpeaks. Figure 11(b) shows that B3 made a total of nine separate collisions with P1 and with B1, a result that is consistent with repeated application of Eqs. (1)–(4). If  $e=0.88$ , then B3 makes nine separate collisions before the two balls separate, with B1 bouncing to 49% of the drop height and B3 bouncing to 28% of the drop height, a result that is in very good agreement with observations for this pair of balls.

A further check on the bounce behavior was made using two nominally identical versions of B1. In addition, a 30 mm length of adhesive copper strip was attached to each ball to measure the contact resistance. For this purpose, the strip on each ball was connected by fine wire to a circuit consisting of a 1.5 V battery and a series resistor. The voltage between the two strips dropped to zero when the two balls made contact. The results are shown in Fig. 12. Using this technique, it was discovered that the two balls lost contact as soon as they were dropped, probably as a direct result of the small force used to hold them together until they were dropped. Being elastic, the two balls presumably bounced slightly apart

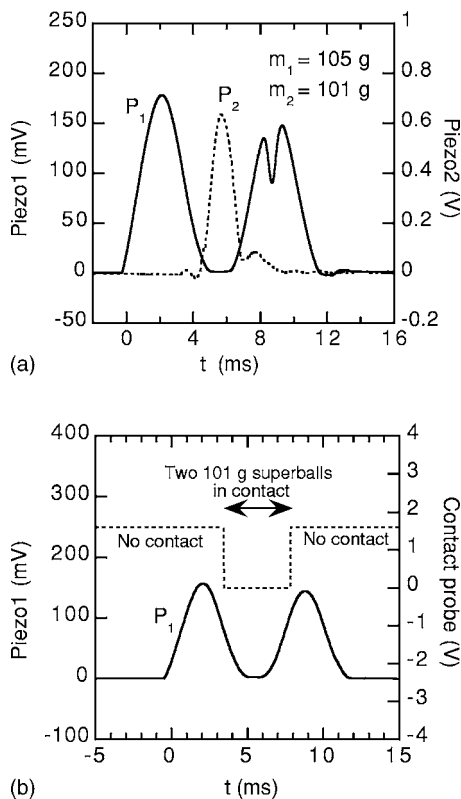


Fig. 12. (a) Force waveforms measured using two large superballs. (b) Result when P2 is replaced by two copper strips to measure the contact resistance between the two balls.

when the force was released. By using only the weight of the top ball to hold the balls together, it was possible to reduce the delay to about 1 ms, in which case the two separate P1 peaks merged into one broad peak with two subpeaks, and the total impact duration shown in Fig. 12 was reduced from 12 to 9 ms.

The result in Fig. 12(a) is described approximately by Eqs. (1) and (2) with  $e=0.88$  in which case the lower ball rebounds with  $e_1=0.75$ , and the upper ball rebounds with  $e_1=0.80$ . In reality, the two balls were observed to rebound at the same speed, indicating that the coefficient of restitution of the lower ball was different for collisions with P1 and with the upper ball, as one would expect. For example, if the coefficient of restitution for a collision off P1 was 0.76 and the coefficient of restitution for a collision between the two balls was 1.0, then the calculated values of  $e_1$  and  $e_2$  are both 0.76, equal to the values in Table II. The dip in the second P1 peak in Fig. 12(a), together with observation of the video, indicates that the two balls maintained rolling contact during the rebound as a result of a slight misalignment of the ball centers.

## V. MASS-SPRING MODEL CALCULATIONS

Two modifications to the simple mass-spring model described in Sec. II are required to give a reasonably good description of the superball results. One is to introduce a small separation  $d$  between the balls as they fall. The other is to account for energy loss in at least one of the balls. Calculations are presented in the following for the two cases where the two small balls were on top of the large ball and where

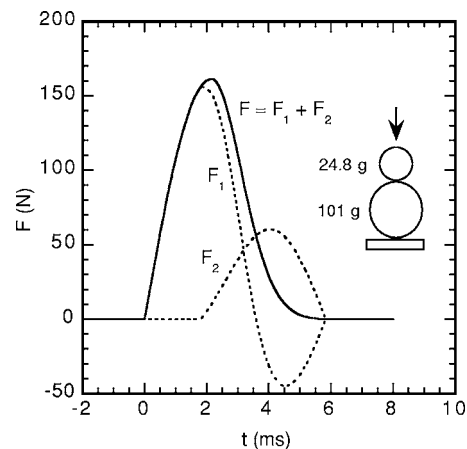


Fig. 13. Mass-spring calculation for the B1-B2 combination assuming that the balls were spaced 1 mm apart as they fell and that the coefficient of restitution of the B1 ball was 0.78. The experimental result is shown in Fig. 10(a) (where P1 is proportional to  $F$ , and P2 is proportional to  $F_2$ ).

hysteresis loss is included in the large ball but not the small balls. To account for hysteresis, we can assume a linear compression of spring  $S_1$  with  $F=k_1x$ , and a nonlinear expansion with  $F=k_3x^n$  and with  $k_3x^n=k_1x$  at maximum compression. In that case, the coefficient of restitution for a collision between the large ball and a rigid surface is given by  $e^2=2/(n+1)$ . Because  $e=0.78$  for the large ball,  $n=2.3$ . The ball separation  $d$  and the spring constants  $k_1$  and  $k_2$  were then chosen to provide a best fit to the experimental results.

The results for the B1-B2 combination are shown in Fig. 13. The best fit was obtained with  $d=1$  mm,  $k_1=5.6 \times 10^4$  N m $^{-1}$ , and  $k_2=1.6 \times 10^4$  N m $^{-1}$  giving  $e_1=0.24$  and  $e_2=1.83$ . The best fit for the B1-B3 combination was obtained with  $d=2.4$  mm,  $k_1=5.4 \times 10^4$  N m $^{-1}$ , and  $k_2=1.4 \times 10^4$  N m $^{-1}$ , giving  $e_1=0.56$  and  $e_2=2.16$ . Both sets of calculations are in reasonably good agreement with the experimental results and with the independent measures of dynamic stiffness for each ball.

The calculations for cases where the large ball was on top of a small ball were qualitatively consistent with the experimental results, but no attempt was made to include energy losses in either ball. The problem here is that each ball undergoes multiple hysteresis cycles, and the nature of the resulting hysteresis curves is not known.

## VI. DISCUSSION AND CONCLUSION

All of the experimental results described in this paper are consistent with an explanation based on the premise that the two balls undergo separate collisions with the floor or with each other before separating. The good agreement with the experimental results is surprising because in most cases, and especially when a tennis ball and basketball are dropped together, this premise is false. Because the impact duration for the basketball collision was 30 ms, a 2 or 3 ms delay in the arrival of the tennis ball means that the two balls maintain close contact throughout most of the collision. The delay could even have been as long as 7 ms in Fig. 8, in which case the two balls maintained contact for at least 23 ms while the basketball was still on the floor. The basketball did not bounce off the floor and then collide with the tennis ball, as is usually assumed. The same can generally be said of the

superball collisions, although two cases were observed [Figs. 11(b) and 12] where the arrival of the upper ball was sufficiently delayed that the lower ball bounced off the floor before colliding with the upper ball.

In the three cases studied with a small ball on top of a large ball, reasonably good fits to the data could also be obtained using the simultaneous collision model, provided that energy loss was included in the calculations and the dynamic stiffness between the two balls was 2.5 to 3.9 times smaller than the stiffness between the lower ball and the rigid surface on which it bounced. The latter result was unexpected but is an essential part of the explanation of the original discrepancy. For the case of colliding masses on an air track, the dynamic stiffness between the two masses is the same as that between the end stop and the mass colliding with it. For a tennis ball on top of a basketball, the tennis ball was much stiffer than the basketball, but it deformed the top of the basketball in such a way that the static stiffness between the two balls was 1.8 times smaller than that at the bottom of the ball. The dynamic stiffness was estimated as being 2.5 times smaller, a result that suggests that the top of a basketball might indent slightly when it impacts on the floor. The dynamic stiffness ratio for superball collisions was found to be about 3.7, a result that can be partially attributed to the difference in the diameters of the two balls, small balls being softer than large balls by the ratio of their diameters. In

addition, the stiffness between two balls is smaller than either ball because the two balls are in series elastically.

<sup>a)</sup>Electronic mail: cross@physics.usyd.edu.au

<sup>1</sup>W. G. Harter, "Velocity amplification in collision experiments involving superballs," *Am. J. Phys.* **39**, 656–663 (1971).

<sup>2</sup>J. S. Huebner and T. L. Smith, "Multi-ball collisions," *Phys. Teach.* **30**, 46–47 (1992).

<sup>3</sup>W. R. Mellen, "Aligner for elastic collisions of dropped balls," *Phys. Teach.* **33**, 56–57 (1995).

<sup>4</sup>S. Redner, "A billiard-theoretic approach to elementary one-dimensional elastic collisions," *Am. J. Phys.* **72**, 1492–1498 (2004).

<sup>5</sup>A difference between sequential and simultaneous collisions is also found when the end stop is replaced by a third glider [L. Flansburg and K. Hudnut, "Dynamical solutions for linear elastic collisions," *Am. J. Phys.* **47**, 911–914 (1979)], or by a group of gliders as in Newton's cradle [F. Hermann and P. Schmalzle, "Simple explanation of a well-known collision experiment," *Am. J. Phys.* **49**, 761–764 (1981)].

<sup>6</sup>P. Patricio, "The Hertz contact in chain elastic collisions," *Am. J. Phys.* **72**, 1488–1491 (2004).

<sup>7</sup>H. Brody, R. Cross, and C. Lindsey, *The Physics and Technology of Tennis* (Racquet Tech Publishing, Solana Beach, 2002).

<sup>8</sup>R. Cross, "The bounce of a ball," *Am. J. Phys.* **67**, 222–227 (1998).

<sup>9</sup>R. Cross, "Dynamic properties of tennis balls," *Sports Eng.* **2**, 23–33 (1999).

<sup>10</sup>R. Hessel, A. C. Perinotto, R. A. M. Alfaro, and A. A. Preschi, "Force-versus-time curves during collisions between two identical steel balls," *Am. J. Phys.* **74**, 176–179 (2006).

#### ALL BACK ISSUES NOW AVAILABLE ONLINE

The contents of the *American Journal of Physics* are available online. AJP subscribers can search and view full text of AJP issues from the first issue published in 1933 to the present. Browsing abstracts and tables of contents of online issues and the searching of titles, abstracts, etc. is unrestricted. For access to the online version of AJP, please visit <http://aapt.org/ajp>.

Institutional and library ("nonmember") subscribers have access via IP addresses to the full text of articles that are online; to activate access, these subscribers should contact AIP, Circulation & Fulfillment Division, 800-344-6902; outside North America 516-576-2270 or [subs@aip.org](mailto:subs@aip.org).

Individual ("member") subscribers to the print version who wish (for an additional fee) to add access to the online version should contact AAPT or go to the AAPT website: <https://www.aapt.org/Membership/secure/agreement.cfm>.